

pubs.acs.org/IECR Article

Separation of Azeotropic Refrigerant Mixtures: R-450A, R-456A, R-515B, and R-516A Using Phosphonium- and Imidazolium-Based Ionic Liquids

Abdulrhman M. Arishi, Julia E. Espinoza Mejia, and Mark B. Shiflett*



Cite This: *Ind. Eng. Chem. Res.* 2024, 63, 6754–6765



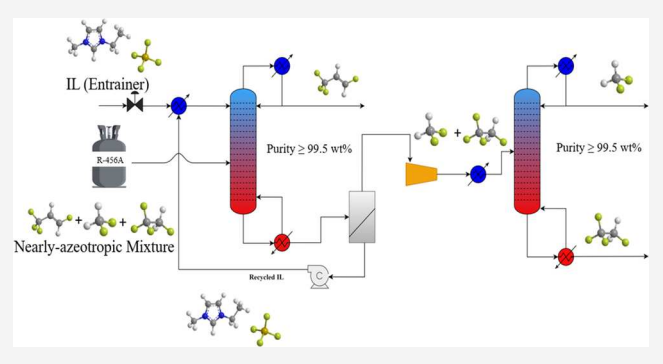
ACCESS I

Metrics & More

Article Recommendations

s Supporting Information

ABSTRACT: Hydrofluorocarbon (HFC) refrigerants are currently being phased down by 85% over the next two decades due to their high global warming potential (GWP). Hydrofluoroolefin (HFO) refrigerants are being commercialized as replacements for HFCs and have significantly lower GWP and zero ozone depletion potential (ODP). A challenge in the transition to HFO refrigerants is compatibility with the existing equipment. One solution is blending HFO and HFC refrigerants to match equipment performance. Several azeotropic refrigerant mixtures, such as R-450A, R-456A, R-515B, and R-516A, have lower GWP and provide similar thermophysical properties to replace HFCs in existing systems. HFO/HFC blends are excellent alternatives that enable



the reduction of HFCs while still maintaining the lifespan of existing equipment. Many HFO/HFC refrigerant mixtures are designed to be azeotropic or near-azeotropic so that if the refrigerant leaks from the system, only a minimal change in composition will occur, which makes servicing the equipment easier. However, this poses a challenge when recycling the refrigerant because conventional distillation cannot be used to separate the HFO/HFC components back into pure products. A proposed solution for separating azeotropic mixtures uses extractive distillation with an ionic liquid (IL) as the entrainer. This novel method offers an efficient means of separating azeotropic refrigerant mixtures. The efficacy of ILs as entrainers is contingent upon their selectivity and strong affinity toward one or more components of the mixture. In addition, the limited availability of solubility data for HFOs and HFCs in ILs constrains the process of selection. This work has identified phosphonium- and imidazolium-based ILs for the separation of four commercial HFO/HFC refrigerant mixtures based on ASPEN Plus simulations.

■ INTRODUCTION

Hydrofluoroolefin (HFO) refrigerants are being developed and commercialized as the next generation of refrigerants that have significantly lower global warming potential (GWP) in comparison to hydrofluorocarbons (HFCs). In 2020, the American Innovation and Manufacturing (AIM) Act was signed by Congress to phase down both the consumption and production of HFCs over the next two decades by 85%. HFOs are considered excellent alternatives to HFCs with minimal environmental impacts (e.g., low GWP, zero ozone depletion potential (ODP), and similar thermodynamic efficiency). However, current equipment designed for HFCs may not be directly compatible with HFOs as drop-in replacements without modifications due to the differences in thermophysical properties, material compatibility (e.g., lubricants), and flammability levels. For instance, HFOs and HFCs have differences in volumetric cooling/heating capacity and the amount of energy produced per unit volume, which could result in different compressor size requirements. Furthermore, current equipment may not be designed for mildly flammable refrigerants (e.g., ASHRAE A2 and A2L category) as the

majority of HFCs are nonflammable (e.g., ASHRAE A1 category); therefore, safety standards must be considered when transitioning to HFOs that are generally classified as mildly flammable. Scientific studies show that some HFO/HFC blends provide similar thermophysical properties as HFCs, which function as near drop-in replacements without significant modifications in some applications. HFO/HFC blends offer a significant decrease in GWP in comparison to HFCs and the blends can be formulated to be nonflammable (Table 1), allowing a smooth transition to HFOs and a gradual reduction in HFC consumption. Some HFO/HFC blends are already on the market (Table 1) and others will be commercialized soon. These blends provide an optimal solution for existing equipment that can have decades of useful life remaining, while future

Received: February 7, 2024 Revised: March 18, 2024 Accepted: March 21, 2024 Published: April 2, 2024





Table 1. Refrigerant Blend Properties

refrigerant name	composition (wt %)	GWP_{100}	flammability level-ASHRAE ³
HFC-134a	100.0% pure component	1300 ^a	A1
R-450A	42.0% HFC-134a 58.0% HFO-1234ze(E)	547 ^b	A1
R-456A	45.0% HFC-134a 49.0% HFO-1234ze(E) 6.0% HFC-32	687 ^c	A1
R-515B	91.1% HFO-1234ze(E) 8.9% HFC-227ea	292 ^b	A1
R-516A	8.5% HFC-134a 77.5% HFO-1234yf 14.0% HFC-152a	142 ^d	A2L

^aGWP listed in the Intergovernmental Panel on Climate Change (IPCC),1996 assessment report. ⁴ Honeywell technical data sheet. ^{5,6} ^cKoura Klea technical data sheet. ⁷ ^dARKEMA Global Web site. ⁸

equipment is designed to be compatible for HFOs. To separate these refrigerant blends, many of which are azeotropic (i.e., vapor and liquid compositions are the same) or near-azeotropic (i.e., bubble and dew point temperatures are very close), new separation technologies are needed. For example, the HFO/HFC blends shown in Table 1 are near-azeotropic (e.g., R-450A and R-456A) and azeotropic (e.g., R-515B and R-516A) that have been developed as suitable drop-in replacements for HFC-134a (1,1,1,2-tetrafluoroethane, CH_2FCF_3).

R-450A is a near-azeotropic mixture consisting of 42.0 wt % HFC-134a and 58.0 wt % HFO-1234ze(E) (trans-1,3,3,3-tetrafluoroethene, CHF = CHCF₃) with a 58% reduction in GWP compared with HFC-134a. Gatarić and Lorbek found that the overall performance was maintained when R-450A was used as a drop-in replacement for HFC-134a in a tumble dryer heat pump, concluding the suitability of R-450A to replace HFC-134a in some applications. In addition, Makhnatch et al. conducted an experimental study for replacement of HFC-134a with R-450A in a small refrigerator and concluded that the overall performance was acceptable for this application. R-450A is supplied by Honeywell.

R-456A is a near-azeotropic mixture consisting of 45.0 wt % HFC-134a, 6.0 wt % HFC-32 (difluoromethane, CH_2F_2), and 49.0% HFO-1234ze(E). In 2023, R-456A became commercially available by Koura to replace HFC-134a with a 50% reduction in GWP.⁷

R-515B is an azeotropic mixture containing 91.1 wt % HFO-1234ze(E) and 8.9 wt % HFC-227ea (1,1,1,2,3,3,3-heptafluor-opropane, CF₃CHFCF₃). Honeywell began selling R-515B in 2020 to replace HFC-134a with a 77% reduction in GWP compared with HFC-134. Mota-Babiloni et al. performed an experimental comparison of R-515B and HFO-1234ze(E) as replacements for HFC-134a in a heat pump. The study confirmed that there was no apparent difference observed using R-515B. Moreover, R-515B may be a more suitable replacement for HFC-134a than HFO-1234ze(E) in certain applications, as it has a nonflammable rating (ASHARE A1 category) that is the same as HFC-134a (ASHRAE A1 category), see Table 1.

R-516A is an azeotropic mixture produced by Arkema, consisting of 8.5% HFC-134a, 14.0% HFC-152a (1,1-difluoroethane, CH₃CHF₂), and 77.5% HFO-1234yf (2,3,3,3-tetrafluoropropene, CH2 = CFCF3).⁸ Kim et al. showed that R-516A has higher energy efficiency compared with other candidates, such as R-513A and HFO-1234ze(E), to replace HFC-134a. Méndez-Méndez et al. also performed an energy evaluation of R-513A and R-516A as a replacement for HFC-134a. R-516A

energy performance was found to be similar to HFC-134a and was recommended for low to medium temperature refrigeration and air-conditioning. Overall, R-516A has the lowest GWP (e.g., 90% reduction) compared with HFC-134a and the other blends shown in Table 1. R-516A also has comparable energy efficiency to that of R-134a, which suggests that this blend may also be a good alternative for both existing and new equipment.

R-513A, which is composed of 44.0 wt % HFC-134a and 56.0 wt % HFO-1234yf produced by Chemours, has a 56% reduction in GWP compared with HFC-134a and an excellent capacity and energy efficiency match with HFC-134a. ¹⁴ In our prior work, we provided results for the separation of this azeotropic refrigerant mixture by extractive distillation and used them as a comparison with this research.

These azeotropic refrigerant blends significantly reduce the GWP compared with HFC-134a, but they pose a challenge when separation is required to recycle the components. Azeotropic refrigerant mixtures have the same vapor and liquid compositions that make difficult to impossible for separating the components using conventional distillation. To break the azeotrope, an entrainer (e.g., solvent) can be used, such that one component has a higher solubility in the solvent at a given temperature (T) and pressure (P) than the other component.

In this work, ionic liquids (ILs) are used as the entrainers (i.e., solvent) in the extractive distillation column. ILs are liquid salts at room temperature with negligible vapor pressures. For example, Zaitsau et al. measured the vapor pressure for 1-ethyl-3-methylimidazolium bis(trifluoromethanesulfonyl)imide ([C₂C₁im][Tf₂N]) to be 6.2×10^{-3} Pa at 441 K and 1-hexyl-3-methylimidazolium bis(trifluoromethylsulfonyl)imide $([C_6C_1im][Tf_2N])$ to be 6.7 × 10⁻³ Pa at 445 K.¹⁵ This negligible vapor pressure for ILs aids in the extraction process when removing the dissolved refrigerants at high T and low P (i.e., under vacuum). In addition, the tunability of the IL is one of the advantages that can be utilized to improve its functionality. For instance, changing the cation or anion of the IL can increase or decrease the solubility and selectivity of the refrigerants in the mixture. 16 Furthermore, the thermal stability of ILs is another advantage over traditional organic solvents. However, the thermal stability can be different from one IL to another based on the choice of cation and anion; therefore, to avoid decomposition, the choice of ILs must take into account the operating conditions of the process. For long-term thermal stability, T_{onset} is not recommended for estimating the thermal stability. To prevent decomposition, users should ensure that the temperatures remain below $T_{0.01/10\,\mathrm{h}}$ (i.e., temperature at which 1% degradation occurs in 10 h). The lower thermal stability of ILs in air is attributed to the presence of oxygen as described by Deferm et al.²⁰ Given the lack of quantifiable thermal stability data for ILs in refrigerants, it is hypothesized that the thermal stability of ILs in refrigerants is similar to that in nitrogen environments, as both lack oxygen.

■ IONIC LIQUID SCREENING

The proper selection of ILs can have a substantial effect on the separation process. Choosing an IL with high selectivity and solubility for one of the components will result in lowering the overall energy demand and minimizing the physical size (i.e., capital costs) for the unit. As a screening process, the selectivity and solubility of refrigerants in ILs are calculated based on vapor—liquid equilibrium (VLE) data for each component of the mixture in the IL (binary system analysis). The minimal solubility data for HFO-1234ze(E) and HFC-

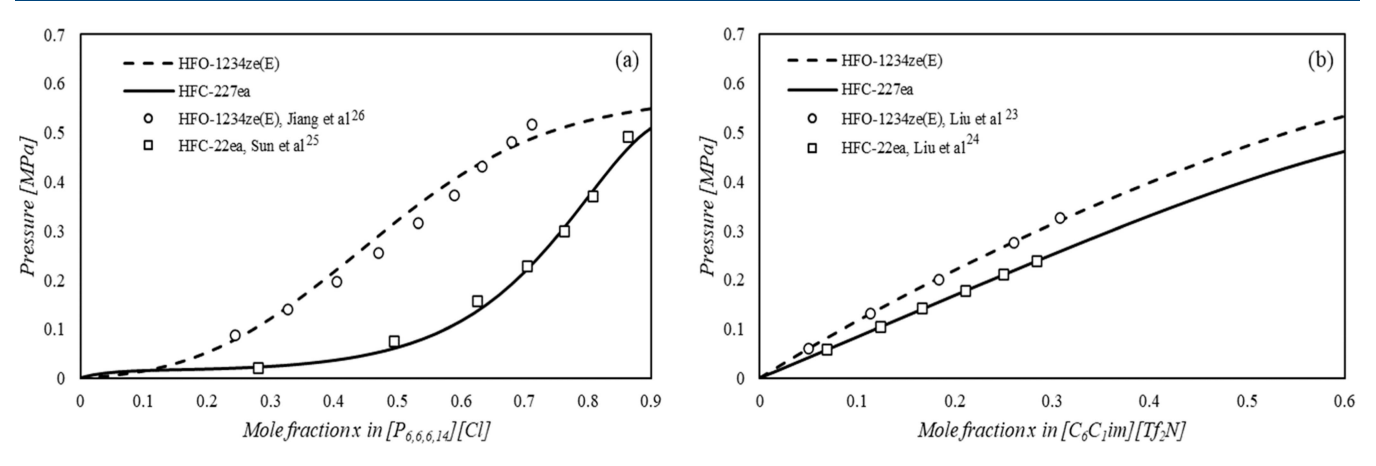
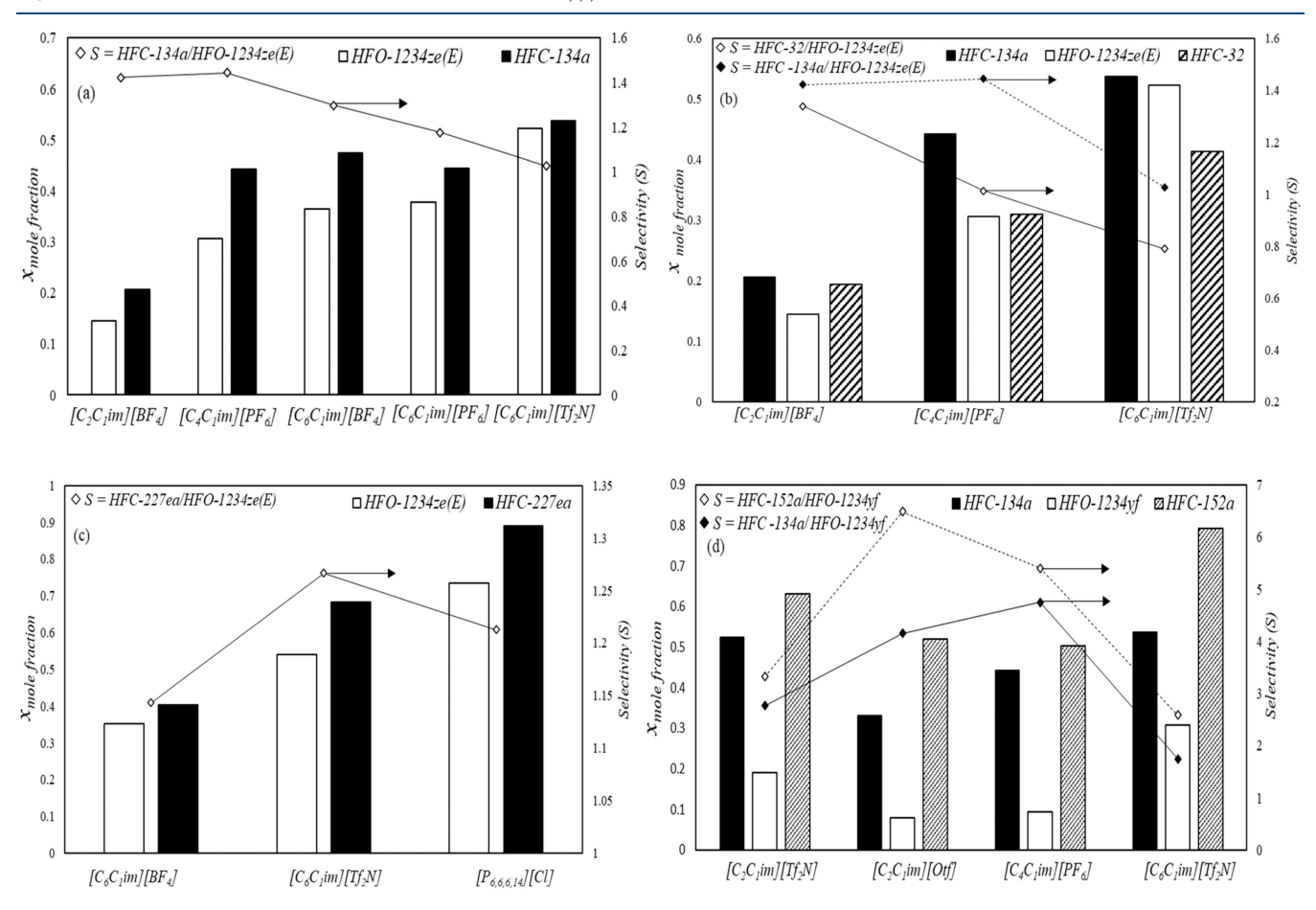


Figure 1. *T-P-x* of HFO-1234ze(E) and HFC-227ea in (a) $[P_{6,6,6,14}][Cl]$ and (b) $[C_6C_1\text{im}][Tf_2N]$ at 303.15 K.



 $\textbf{Figure 2.} \ \ \text{Solubility and selectivity of (a) } \ \ \text{R-450A, (b) } \ \ \text{R-456A, (c) } \ \ \text{R-515B, and (d) } \ \ \text{R-516A at } \ \ 303.15 \ \ \text{K and } \ \ 0.5 \ \ \text{MPa.}$

227ea in ILs constrain the selection of an appropriate IL. Experimentalists and modelers should consider measuring and calculating the solubility of HFO-1234ze(E) in additional ILs. In the case of R-515B, only three ILs were found in the literature with solubility data for the constituent components HFC-227ea and HFO-1234ze(E). Notably, trihexyltetradecylphosphonium chloride $[P_{6,6,6,14}][Cl]$ and $[C_6C_1\text{im}][Tf_2N]$ exhibit similar selectivity of about 1.2 at 303.15 K and 0.5 MPa. $^{23-26}$ However, the selectivity for $[P_{6,6,6,14}][Cl]$ exhibits an increase at lower pressures, as shown in Figure 1. Consequently, $[P_{6,6,6,14}][Cl]$ was selected to be modeled as an entrainer for the separation of R-515B.

In the case of R-450A, 1-ethyl-3-methylimidazolium tetra-fluoroborate, $[C_2C_1\text{im}][BF_4]$, and 1-butyl-3-methylimidazolium hexafluorophosphate, $[C_4C_1\text{im}][PF_6]$, have a similar selectivity of 1.4 at 303.15 K and 0.5 MPa (Figure 2), which is considered a low selectivity but has the highest value among the five known ILs with available solubility data for R-450A constituent components, HFC-134a and HFO-1234ze(E). Viar et al. prioritize low-viscosity ILs in addition to high selectivity as part of the screening process. This work is based on a simulation using an equilibrium model; therefore, viscosity does not play a role in the results. If a rate-based model is considered, then the transport properties, such as viscosity,

density, and surface tension, must be included, and the higher the viscosity of the IL, potentially the lower the mass transport. However, the amount of refrigerant dissolved in the IL will decrease the viscosity, which also plays an important role and can increase the mass transport. The viscosities of $[C_2C_1\mathrm{im}]$ - $[BF_4]$ and $[C_4C_1\mathrm{im}]$ - $[PF_6]$ are 0.0434 \pm 0.0047 and 0.37 \pm 0.1 Pa·s, respectively, at 293 K and 0.1 MPa. 28,29 In the case of R-450A, $[C_2C_1\mathrm{im}]$ - $[BF_4]$ is chosen for the simulation because it has a slightly lower viscosity compared with $[C_4C_1\mathrm{im}]$ - $[PF_6]$, but this has no impact on the equilibrium-based simulation shown in this work.

In the case of the ternary mixture R-456A, the binary pair of HFC-134a and HFO-1234ze(E) forms an azeotrope, and HFC-32 does not form an azeotrope with either HFC-134a or HFO-1234ze(E). In this case, $[C_2C_1im][BF_4]$ is an optimal choice, with a selectivity of 1.4 for HFC-134a in the HFC-134a/ HFO-1234ze(E) mixture. Also, based on the HFC-32/HFO-1234ze(E) mixture in the same IL, the selectivity for HFC-32 is almost the same, 1.34 at 303.15 K and 0.5 MPa, as shown in Figure 2. Also, HFC-32 and HFC-134a exhibit similar solubilities in $[C_2C_1im][BF_4]$ at the same T and P. In this simulation, the IL [C₂C₁im][BF₄] will preferentially dissolve HFC-32 and HFC-134a and the HFO-1234ze(E) will be concentrated in the distillate. HFC-32 and HFC-134a can be separated from the IL using heat and vacuum, and the two refrigerants can be further separated using traditional fractional distillation since no azeotrope exists for this binary pair.

The azeotropic ternary mixture R-516A has two components, HFC-134a and HFC-152a, which exhibit azeotrope-like behavior, and both form azeotropes with the third component of the mixture, HFO-1234yf. In this case, the separation of the mixture into three pure compounds required the use of two solvents. As illustrated in Figure 2, HFC-134a and HFC-152a show higher solubility in $[C_4C_1\text{im}][PF_6]$ compared to HFO-1234yf; therefore, $[C_4C_1\text{im}][PF_6]$ is used to extract HFO-1234yf. The remaining components, HFC-134a and HFC-152a, exhibit different solubilities in $[C_2C_1\text{im}][OTF]$, which is chosen as the second entrainer to separate these refrigerants.

The IL selection is constrained by the available experimental data. Asensio-Delgado et al. proposed a useful method to predict the solubility in ILs using a prescreening tool based on an artificial neural network (ANN).³⁶ However, the high polarity of refrigerants, such as HFC-227ea (CHF₂CF₂CF₃), led to inaccurate predictions using the ANN; therefore, experimental solubility measurements are needed for HFC-227ea and HFO-1234ze(E) in different ILs that have a higher solubility difference (i.e., higher selectivity) between these components. In particular, experimental data for HFO-1234ze(E) are critically needed because it is being used in multiple HFO/HFC refrigerant blends, including R-450A, R-456, and R-515B. HFO-1234ze(E) is one of the next-generation refrigerants being commercialized, and in order to separate it from azeotropic mixtures containing HFCs, additional solubility data as a function of T and P are required. Molecular simulations are also needed to help with the selection of ILs to maximize solubility and selectivity for HFO-1234ze(E) combined with other refrigerants.

■ THERMODYNAMIC MODEL

The Peng–Robinson–Boston–Mathias (PR-BM) property method in ASPEN Plus V11 was used to model and predict the phase equilibria data for refrigerants and ILs using the Peng–

Robinson equation of state (PR EOS) and the Boston–Mathias mixing rule.

$$P = \frac{RT}{V_m - b} - \frac{a}{V_m (V_m + b) + b (V_m - b)}$$
(1)

where

$$b = \sum_{i} x_{i} b_{i} \tag{2}$$

A linear mixing rule for parameter b

$$a = a_0 + a_1 \tag{3}$$

Parameter a is given by summation of a_0 quadratic term and a_1 , an additional asymmetric (polar) term, as proposed by Mathias et al.³⁷

$$a_0 = \sum_{i} \sum_{j} x_i x_j (a_i a_j)^{0.5} (1 - k_{ij})$$
(4)

$$k_{ij} = k_{ij}^{(1)} + k_{ij}^{(2)}T + \frac{k_{ij}^{(3)}}{T}$$
 (5)

 $k_{ij} = k_{ji}$

$$a_1 = \sum_{i=1}^n x_i \left(\sum_{j=1}^n x_j \left((a_i a_j)^{1/2} l_{ij} \right)^{1/3} \right)^3$$
 (6)

$$l_{ij} = l_{ij}^{(1)} + l_{ij}^{(2)}T + \frac{l_{ij}^{(3)}}{T}$$
(7)

Generally

$$l_{ii} \neq l_{ii}$$

The a_i and b_i are pure component parameters used in the PR EOS that can be calculated using eqs 8 and 9.³⁸

$$a_i = \alpha_i 0.45724 \frac{R^2 T_c^2}{P_c} \tag{8}$$

$$b_i = 0.07780 \frac{RT_c}{P_c} \tag{9}$$

$$\alpha_i(T) = [1 + m_i(1 - T_r^{1/2})]^2 \tag{10}$$

where m_i is the parameter correlated to the acentric factor (ω) and is given by the following expression

$$m_i = 0.37464 + 1.54226\omega_i - 0.26992\omega_i^2 \tag{11}$$

Boston and Mathias derived an alternative α function for temperatures above the critical T because eq 11 will provide unrealistic results at high reduced T.

$$\alpha_i(T) = [\exp(c_i(1 - T_c^{d_i}))]^2$$
 (12)

where

$$c_i = 1 - \frac{1}{d_i} \tag{13}$$

$$d_i = 1 + \frac{m_i}{2} \tag{14}$$

Using the PR EOS with the Boston–Mathias α function and modified mixing rule including the added asymmetric term will

Table 2. Regression Summary for PR-BM Binary Interaction Parameters a,b

									average absolute deviation			
(i)	(j)	$N_{ m E}$	$N_{ m T}$	temperature range (K)	$k_{ij}^{(1)}$	$k_{ij}^{(2)}$	$l_{ij}^{(1)}$	$l_{ij}^{(2)}$	T (K)	P (MPa)	x_i	references
HFC-134a	$\begin{bmatrix} C_2C_1 im \\ BF_4 \end{bmatrix}$	36	5	283.15-323.15	-0.1070	0.0005	-0.1197	0.0002	0.0870	0.0007	0.003	41
HFO-1234ze(E)		49	7	283.15-343.15	-0.0045	0.0002	0.2159	-0.0008	0.0736	0.0005	0.001	42
HFC-134a	$\begin{bmatrix} C_4C_1im \\ PF_6 \end{bmatrix}$	31	4	283-348.2	-0.2237	0.0008	-0.7527	0.0019	0.0154	0.0789	0.004	43
LLE		3	3	318.2-355					0.0000	6.3067	0.021	44
HFO-1234ze(E)		42	7	283.15-343.15	-0.0937	0.0007	0.1186	-0.0003	0.0216	0.0002	0.001	23
HFC-134a	$\begin{bmatrix} C_6C_1im \\ TF_2N \end{bmatrix}$	40	4	298.15-348.15	0.1807	-0.0006	-0.2093	0.0006	0.0001	0.1902	0.001	45
HFO-1234ze(E)		35	7	293.15-353.15	0.1149	-0.0003	0.5926	-0.0020	0.0000	0.0533	0.000	23
HFC-134a	$\begin{bmatrix} \text{C}_6\text{C}_1\text{im} \\ \text{BF}_4 \end{bmatrix}$	16	3	298-348	-0.0926	0.0003	0.8377	-0.0029	0.0000	0.3089	0.113	45
HFO-1234ze(E)		49	7	283.15-343.15	-0.0437	0.0003	0.0527	-0.0002	0.0427	0.0002	0.001	46
HFC-134a	$\begin{bmatrix} C_6C_1im \\ PF_6 \end{bmatrix}$	21	3	298-348	-0.0406	0.0003	0.0236	-0.0005	0.1169	0.0031	0.008	45
HFO-1234ze(E)		42	7	283.15-343.15	-0.0792	0.0006	0.0899	-0.0003	0.0302	0.0002	0.001	47

 $^{^{}a}N_{E}$ = Number of experimental data point. N_{T} = Number of temperatures at which measurements were conducted at refrigerant mixture R-450A. b PR-BM binary interaction parameters for R-456A, R-515B, and R-516A are provided in the Supporting Information.

Table 3. Physical and Critical Properties for ILs and Refrigerants Used in This Work^{a, 50,51}

name	formula	$MW \ (g \ mol^{-1})$	$T_{b}(K)$	$T_{c}(K)$	$P_{\rm c}$ (MPa)	$V_{\rm c}~({\rm cm}^3~{\rm mol}^{-1})$	$Z_{\rm c}$	Ω			
$[C_2C_1im][BF_4]$	$C_6H_{11}N_2BF_4$	197.97	449.5	1234.4	2.36	540	0.2573	0.8087			
$[C_2C_1im][OTF]$	$C_7H_{11}F_3N_2O_3S$	260.23	662	992.3	3.58	636.4	0.2765	0.3255			
$[C_2C_1im][Tf_2N]$	$C_8H_{11}N_3F_6S_2O_4$	391.3	816.7	1249.3	3.27	875.9	0.2753	0.2157			
$[C_4C_1im][PF_6]$	$C_8H_{15}N_2PF_6$	284.2	554.6	719.4	1.73	762.5	0.2203	0.7917			
$[C_6C_1im][BF_4]$	$C_{10}H_{19}BF_4N_2$	254.08	541	1080.6	1.79	769.2	0.2406	0.9625			
$[C_6C_1im][PF_6]$	$C_{10}H_{19}F_6N_2P$	312.24	600.3	764.9	1.55	876.7	0.2137	0.8697			
$[C_6C_1im][Tf_2N]$	$C_{12}H_{19}N_3F_6S_2O_4$	447.41	908.2	1292.8	2.39	1104.4	0.2454	0.3893			
[P _{6,6,6,14}][Cl]	$C_{32}H_{68}PCl$	519.3	1006.2	1222.8	0.79	2002.2	0.1565	0.7947			
HFC-32	CH_2F_2	52.02	221.46	351.28	5.78	122.4	0.24233	0.2766			
HFC-134a	$C_2H_2F_4$	102.03	247.08	374.18	4.06	199	0.26103	0.32695			
HFC-152a	$C_2H_4F_2$	66.05	249.15	386.44	4.51	179	0.25165	0.27524			
HFC-227ea	C_3HF_7	170.03	256.76	375.01	2.93	291.5	0.27384	0.356			
HFO-1234yf	$C_3H_2F_4$	114.04	243.65	367.85	3.38	240	0.32695	0.2753			
HFO-1234ze(E)	$C_3H_2F_4$	114.04	254.203	382.51	3.63	233	0.268	0.31313			
^a HFCs and HFOs data obtained from the NIST database.											

enable the modeling of polar and nonideal chemical systems. Maqbool et al. found PR-BM to be ideal for fitting solubility data and representing the binary phase behavior for systems when at least one component is polar. This model enables precise predictions of phase behavior under specified T and P conditions, facilitating the evaluation of selectivity and solubility in the absence of isothermal vapor—liquid equilibrium (VLE) and liquid—liquid equilibrium (LLE) data at particular T and P conditions. In this work, the ideal selectivity for the binary

systems was calculated using the following expression

$$S_{ij}(T, P) = \left(\frac{x_i}{x_j}\right) \tag{15}$$

where subscripts "i" and "j" refer to the component i (i.e., HFC) and component j (i.e., HFO), and x is the mole fraction of the dissolved refrigerant in ILs.

PR-BM has accurately described the phase behavior of the IL/refrigerant binary systems with a low average absolute difference (AAD) between calculated and experimental values for *PTx*, as shown in Table 2, for R-450A.

The maximum-likelihood objective function was used in ASPEN Plus for VLE and LLE regression and is listed in eq 16.

$$Q = \sum_{d=1}^{D} w \sum_{n=1}^{NP} \left[\left(\frac{T^{\text{est}} - T^{\text{exp}}}{\sigma_{T,n}} \right)^{2} + \left(\frac{P^{\text{est}} - P^{\text{exp}}}{\sigma_{p,n}} \right)^{2} + \sum_{i=1}^{NC-1} \left(\frac{x^{\text{est}} - x^{\text{exp}}}{\sigma_{x,n,i}} \right)^{2} + \sum_{i=1}^{NC-1} \left(\frac{y^{\text{est}} - y^{\text{exp}}}{\sigma_{y,n,i}} \right)^{2} \right]$$
(16)

The variable (Q) represents the objective function, where (D) denotes the number of data groups, (w) indicates the weight of the data group, (NP) represents the number of data points in group d, (NC) denotes the number of components in the data group, and (σ) indicates the standard deviation of the given data. The superscript (est) is the estimated properties and (\exp) is the actual experimental measurements. (P), (T), (x), and (y) are pressure, temperature, liquid, and vapor mole fractions, respectively.

The objective function is minimized by manipulating the estimated values corresponding to each measurement and is

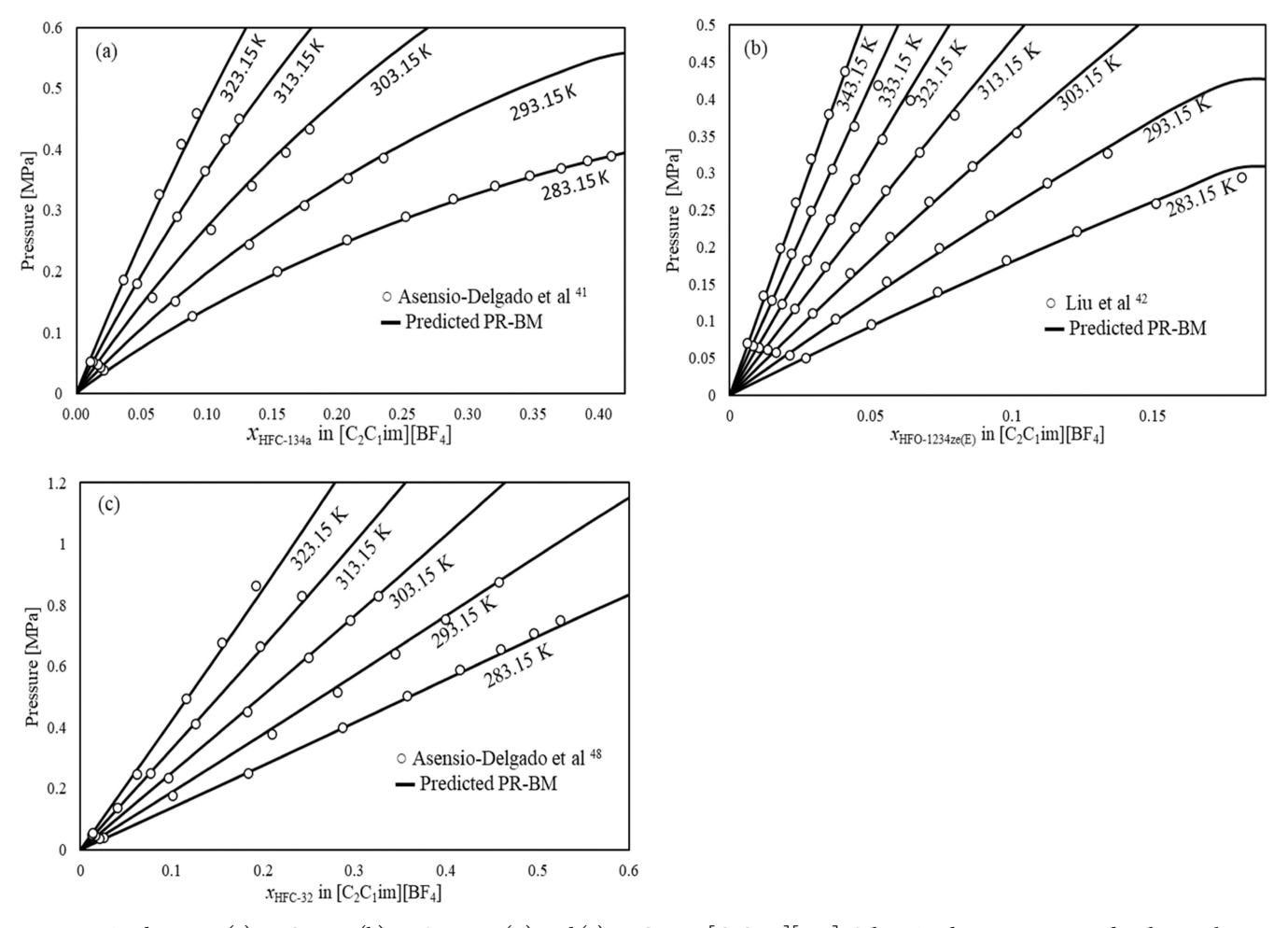


Figure 3. PTx diagrams: (a) HFC-134a, (b) HFO-1234ze(E), and (c) HFC-32 in $[C_2C_1\text{im}][BF_4]$. Other PTx diagrams in ILs used in the simulations are provided in the Supporting Information.

subjected to the constraints of phase equilibrium criteria of VLE and LLE, where the fugacity in each phase is equal.

The PR-BM model was in good agreement with the experimental PTx data of HFOs and HFCs. The regression requires the critical properties of both refrigerants and ILs, which are provided in Table 3, and the ideal gas heat capacity of ILs, which was estimated using the extended Joback method.

The PTx diagrams for HFC-134a, HFO-1234ze(E), and HFC-32 in the IL $[C_2C_1\text{im}][BF_4]$ are shown in Figure 3. HFC-134a and HFO-1234ze(E) are components of R-450A. HFC-134a, HFO-1234ze(E), and HFC-32 are components of R-456A.

SIMULATION

ASPEN Plus V11 was used to perform the simulation for separating the azeotropic refrigerant mixtures. ASPEN Plus enables simulations using either equilibrium- or rate-based models. The equilibrium-based model is typically the method used to begin evaluating a separation and requires equilibrium data (e.g., VLE and LLE). A rate-based model requires mixture transport properties (e.g., viscosity and surface tension) in addition to the physical structure of the distillation column (e.g., packing material, column diameter, column height, etc.).

The extractive distillation process is designed to separate the refrigerant mixture based on the difference in solubility of one refrigerant versus another in the IL. The solvent stage (N_S) is set to be the second stage in all cases to ensure the IL contacts all

stages in the column.⁵² This will increase the contact time between the IL and refrigerant, enhancing the separation process. In addition, the distillate rate (D) is assumed to be equal to the light component fraction multiplied by the total mixture feed flow rate $(D = x_i F)$. Other parameters, such as solvent-tofeed (S/F) ratio, operating P, the number of stages (N_T) , feed stage (N_F) , and reflux ratio (RR), were adjusted using sensitivity analysis in ASPEN Plus. A similar approach for setting the constants and adjusting the manipulated variables was considered in the previous work. ^{22,53,54} The bottom stream of the extractive distillation consists of the refrigerant dissolved in the IL. A flash process that operates at high T and low P (i.e., vacuum) is used to remove the refrigerant from the IL and the IL is recycled back to the top of the column. The flash tank operates at zero heat duty (i.e., no heat added or removed during the process), which involves a phase change, where high P refrigerant liquid is rapidly depressurized, resulting in vaporization of the dissolved gas in the IL. The heat from the reboiler liquid entering the flash provides enough energy, such that the overall energy demand of the process can be minimized. The flash tank is operated under adiabatic conditions, where the reduction in T of the flash tank (T_{flash}) is attributed to the desorption energy and adiabatic expansion of the refrigerant in the tank. However, the low mass fraction of the refrigerants in the bottom stream diminishes the effect of the energy of desorption and refrigerant expansion, resulting in a slight reduction in $T_{\rm flash}$ for R-450A, R-456A, and R-515B. In contrast,

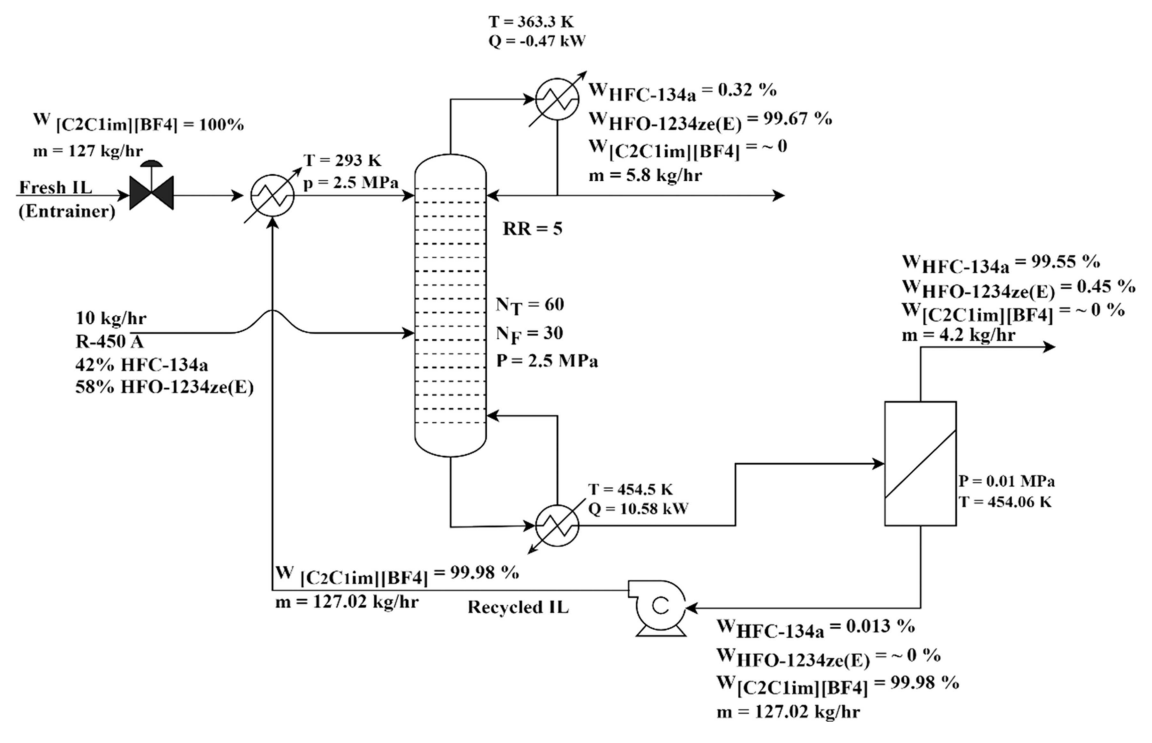


Figure 4. ASPEN Plus PFD for separating R-450A using [C₂C₁im][BF₄].

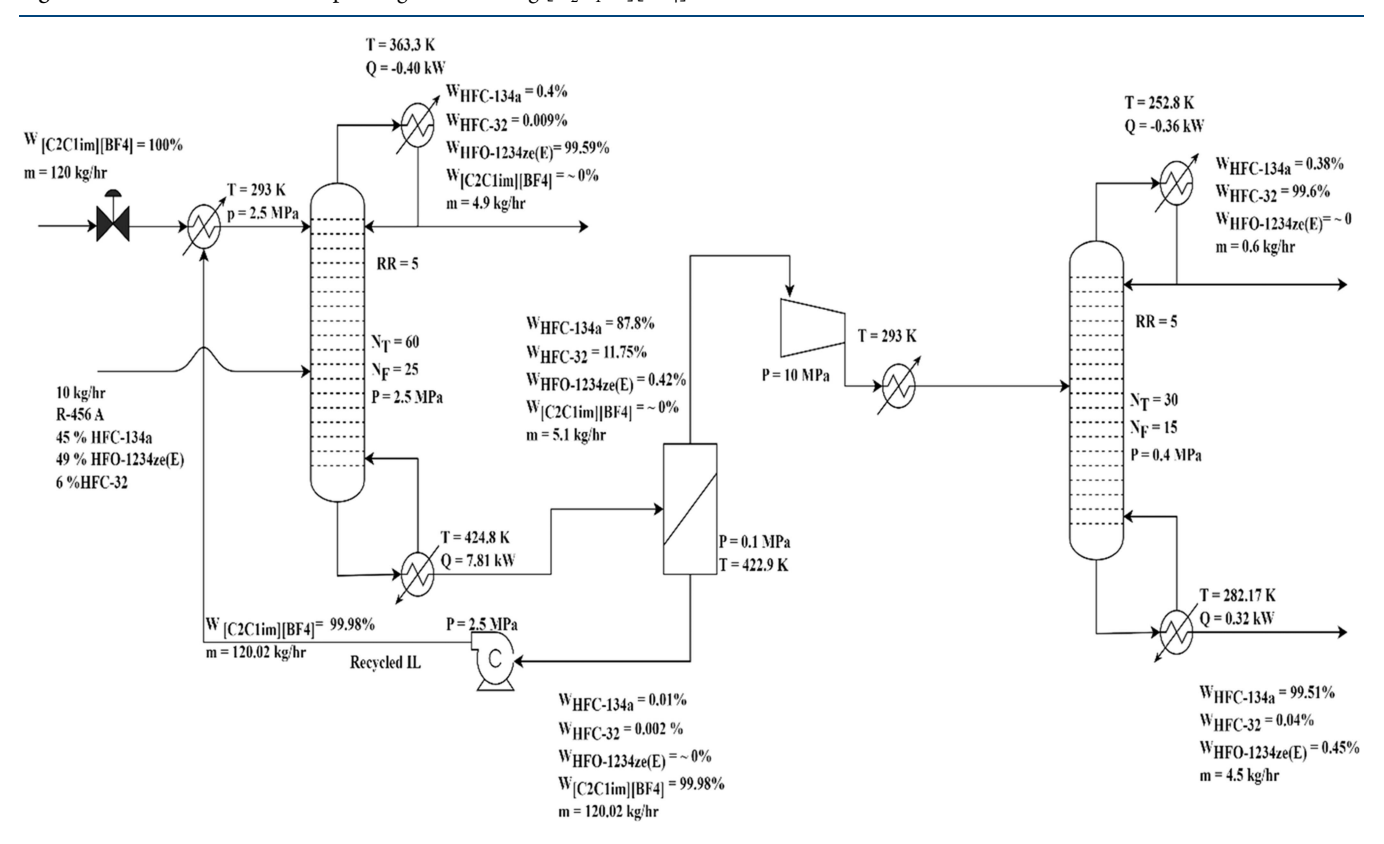


Figure 5. ASPEN Plus PFD for separating R-456A by using $[C_2C_1\text{im}][BF_4]$.

R-516A exhibits a 11.9 K reduction in the first flash and a 7.4 K reduction in the second flash, where the mass fractions of the refrigerant in the inlet flash streams (i.e., bottom stream of distillation column) are 10.5 and 7.3 wt %, respectively.

R-450A Separation. The IL $[C_2C_1\text{im}][BF_4]$ was selected to separate R-450A into HFC-134a and HFO-1234ze(E). In this

separation, HFO-1234ze(E) has a lower solubility in the IL than HFC-134a; therefore, HFO-1234ze(E) is the distillate product and HFC-134a dissolved in the IL is the bottom product, as shown in Figure 4. The bottom stream containing HFC-134a and IL is separated using a flash tank, where the gas is extracted under vacuum, and the IL is recycled back to the column. The

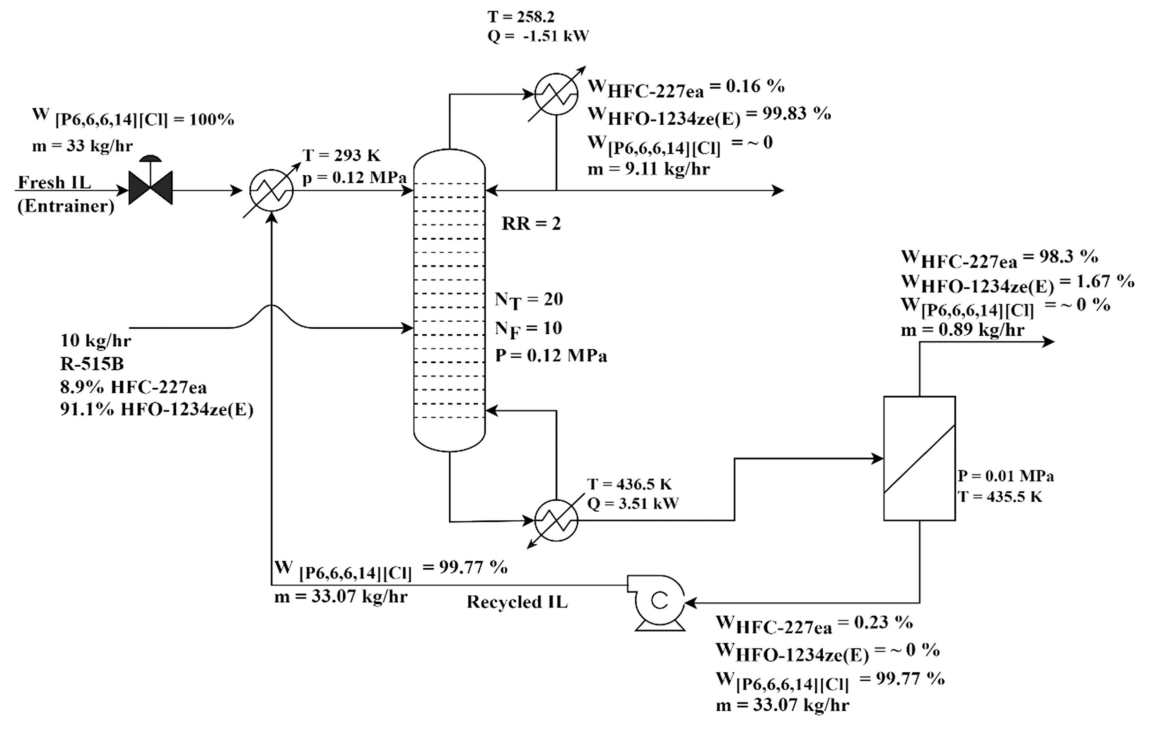


Figure 6. ASPEN Plus PFD for separating R-515B using [P_{6,6,6,14}][Cl].

low vapor pressure for the IL (i.e., $1 \times 10^{-3} - 1 \times 10^{-5}$ Pa) allows the refrigerant to be separated with no loss of IL, which makes ILs uniquely suited for this application.

R-450 can be separated in HFO-1234ze(E) and HFC-134a using $[C_2C_1\text{im}][BF_4]$ with both refrigerants achieving a purity of \geq 99.5 wt % under the following operation conditions ($F=10\,\text{kg/h}$, RR=5, S/F=12.7, $T_{\text{reboiler}}=454.5$ K, $P_{\text{column}}=2.5$ MPa (25 bar), $P_{\text{flash}}=0.01$ MPa (0.1 bar), and $T_{\text{flash}}=454.1$ K). The IL $[C_2C_1\text{im}][BF_4]$ has good thermal stability (e.g., $T_{0.01/10\,\text{h}}=490\,\text{K})^{55}$ and the operating T for the reboiler and flash is well below this threshold. The energy required to operate the process includes the reboiler (10.58 kW), the column condenser ($-0.47\,\text{kW}$), the recycled stream cooler ($-9.9\,\text{kW}$), and the pump (0.36 kW) with a total absolute energy input of 21.31 kW/10 kg/s refrigerant flow rate (2.131 kJ/kg R-450A), which is reasonable for a refrigerant separation process.

R-456A Separation. The IL $[C_2C_1\text{im}][BF_4]$ was selected to extract HFO-1234ze(E) from the ternary mixture R-456A due to the high solubility of both HFC-32 and HFC-134a in $[C_2C_1\text{im}][BF_4]$. The high solubility of HFC-134a and HFC-32 in $[C_2C_1\text{im}][BF_4]$ will break the azeotrope with HFO-1234ze(E). The HFC-134a and HFC-32 can be extracted from the IL using a flash tank, and the IL can be recycled back to the extractive distillation column as shown in Figure 5. The HFC-32 and HFC-134a are pressurized to 1.0 MPa and cooled to 293 K and fed to the fractional distillation column, where the refrigerants are separated based on the difference in boiling points.

The highly efficient separation of the ternary mixture R-456A into pure components (purity of \geq 99.5 wt %) can be achieved using extractive distillation and fractional distillation. The extractive distillation process operates at F=10 kg/h, RR=5, S/F=12, $T_{\rm reboiler}=467.3$ K, $P_{\rm column}=2.5$ MPa (25 bar), $P_{\rm flash}=0.01$ MPa (0.1 bar), $T_{\rm flash}=422.9$ K, $N_{\rm F}=25$, and $N_{\rm T}=60$. The fractional distillation process operates at RR=5, $T_{\rm reboiler}=282.17$ K, $T_{\rm condenser}=252.8$ K, $P_{\rm column}=0.4$ MPa (4 bar), $N_{\rm F}=15$,

and $N_{\rm T}=30$. The overall energy demand of the extractive distillation to extract HFO-1234ze(E), including the reboiler (7.81 kW), the condenser (-0.4 kW), the recycled stream cooler (-7.4 kW), and the pump work (0.33 kW), is 15.94 kW. The overall energy demand of the fractional distillation for separating HFC-32 and HFC-134a, including the reboiler (0.32 kW), the condenser (-0.36 kW), the inlet stream cooler (-0.89 kW), and inlet gas compression work (0.42 kW), is 1.99 kW. The total energy input, including both extractive and fractional distillations, for separating R-456A into pure components, is 17.93 kW/10 kg/s refrigerant flow rate (1.793 kJ/kg R-456A).

R-515B Separation. The IL $[P_{6,6,6,14}][Cl]$ was selected for the separation of R-515B. The selectivity of $[P_{6,6,6,14}][Cl]$ increases at lower P; therefore, the process was designed to operate with $P_{\text{column}}=0.12$ MPa (1.2 bar), RR=2, S/F ratio = 3.3, $T_{\text{reboiler}}=436.5$ K, $T_{\text{condenser}}=258.2$ K, $N_{\text{F}}=10$, and $N_{\text{T}}=20$. The distillate product containing HFO-1234ze(E) achieved a purity of 99.83 wt %. The purity of HFC-227ea in the flash tank operating at $P_{\text{flash}}=0.01$ MPa (0.1 bar) and $T_{\text{flash}}=435.5$ K achieved a purity of 98.3 wt % as shown in Figure 6. The T_{reboiler} operates at 436.5 K, which is close to the thermal stability temperature limit for $[P_{6,6,6,14}][Cl]$ found in the literature (e.g., 438 K).

The overall energy demand of the separation process includes the reboiler (3.51 kW), the condenser (-1.51 kW), the recycle stream cooler (-2.50 kW), and the pump work (0.005 kW) for a total of 7.52 kW/10 kg/s refrigerant flow rate (0.752 kJ/kg R-515B).

The purity of HFC-227ea can be slightly improved at higher pressures between 0.13 and 0.5 MPa; however, the IL may not be thermally stable with $T_{\rm reboiler} = 444.8-570.4$ K at those corresponding $P_{\rm column}$.

R-516A Separation. The R-516A separation requires two consecutive extractive distillations with different IL entrainers. The IL $[C_4C_1\text{im}][PF_6]$ is selected as the entrainer in the first extractive distillation to distill HFO-1234yf by entraining HFC-

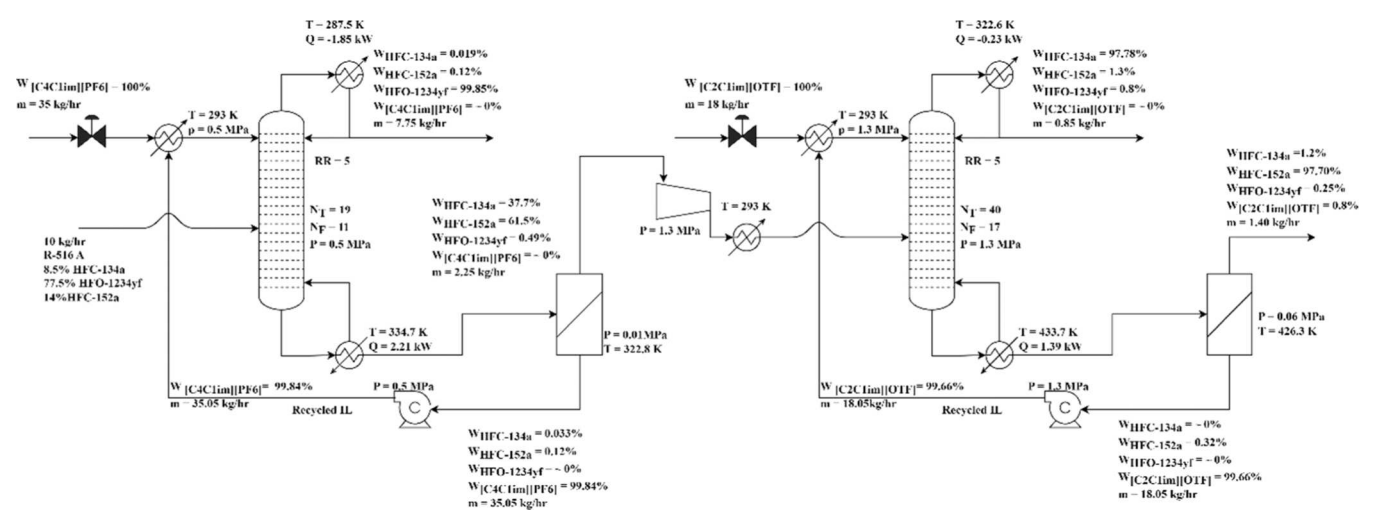


Figure 7. ASPEN Plus PFD for separating R-516A using $[C_4C_1\text{im}][PF_6]$ and $[C_2C_1\text{im}][OTF]$.

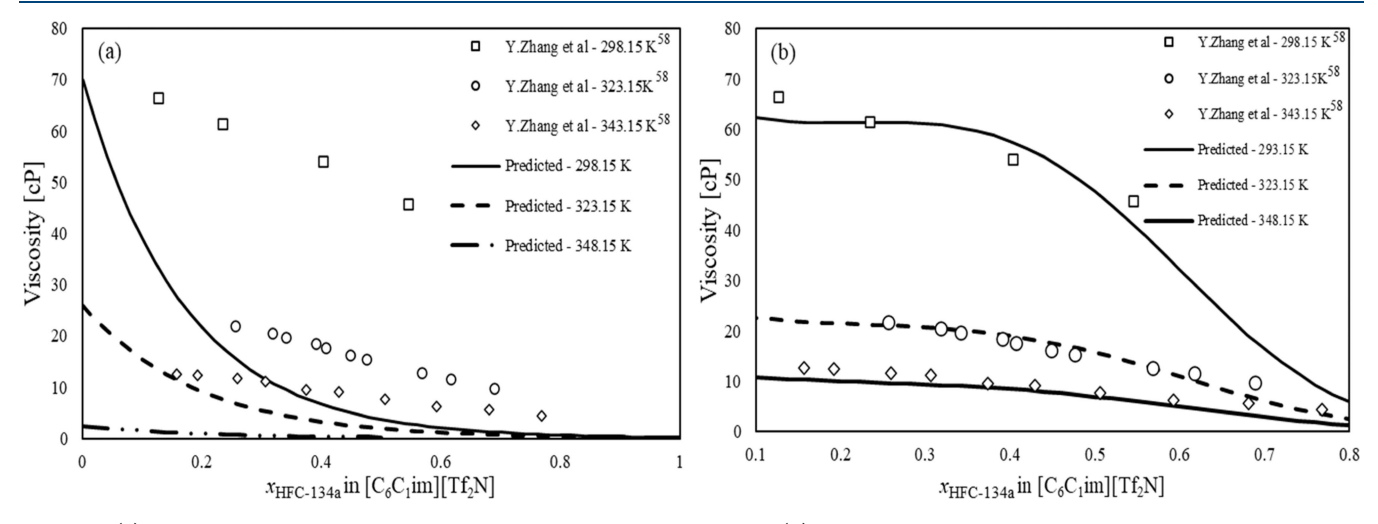


Figure 8. (a) ASPEN Plus viscosity model estimation without experimental data. (b) ASPEN Plus model estimation based on experimental data regression using the liquid mixture viscosity model (the model is provided in the Supporting Information).

134a and HFC-152a. A flash vessel is used to desorb HFC-134a and HFC-152a from the IL. HFC-134a and HFC-152a are nearly azeotropic with similar boiling points and have to be separated based on the difference in solubility using IL 1-ethyl-3-methylimidazolium trifluoromethanesulfonate $[C_2C_1\text{im}][OTF]$ as shown in Figure 7.

To achieve the targeted purity of ≥99.5 wt % for HFO-1234ze(E) and recycle IL $[C_4C_1im][PF_6]$, the following operating conditions were required: S/F ratio = 3.5, P_{column} = 0.5 MPa, $N_{\rm F}$ = 11, $N_{\rm T}$ = 19, $T_{\rm reboiler}$ = 334.7 K, $T_{\rm condenser}$ = 287.5 K, $P_{\text{flash}} = 0.01$ MPa (0.1 bar), and $T_{\text{flash}} = 322.8$ K. The refrigerants HFC-134a and HFC-152a were separated in the flash vessel, pressurized to 1.3 MPa, cooled to 293.15 K, and fed to the second extractive distillation. The purities for HFC-134a and HFC-152a were approximately 97 wt % at the following operating conditions: S/F ratio = 8, P_{column} = 1.3 MPa, N_{F} = 17, $N_{\rm T}$ = 40 $T_{\rm reboiler}$ = 433.7 K, $T_{\rm condenser}$ = 322.6 K, $P_{\rm flash}$ of 0.06 MPa (0.6 bar), and $T_{\text{flash}} = 426.3$ K. The overall absolute energy demand for the separation process, which includes the reboilers, condensers, coolers, pump, and compressor for both extractive distillation columns, is 7.62 kW/10 kg/s refrigerant flow rate (0.762 kJ/kg R-516A).

The $T_{0.01/10\,\mathrm{h}}$ of $[\mathrm{C_4C_1im}][\mathrm{PF_6}]$ is 521 K. The $T_{0.01/10\,\mathrm{h}}$ of $[\mathrm{C_2C_1im}][\mathrm{OTF}]$ is unknown, but with the same cation ($[\mathrm{C_2C_1im}]$), the $T_{0.01/10\,\mathrm{h}}$ with the anion $[\mathrm{OTF}]$ is higher than $[\mathrm{HSO_4}]$ and lower than $[\mathrm{BF_4}]$ as described by Cao et al. The maximum operation T for less than 1% loss of $[\mathrm{C_2C_1im}][\mathrm{HSO_4}]$ per month is 454 K according to Heym et al. Short $T_{0.01/10\,\mathrm{h}}$ for $[\mathrm{C_2C_1im}][\mathrm{OTF}]$ is higher than 454 K (i.e., $T_{0.01/10\,\mathrm{h}}$ of $[\mathrm{C_2C_1im}][\mathrm{HSO_4}]$) and lower than 490 K (i.e., $T_{0.01/10\,\mathrm{h}}$ of $[\mathrm{C_2C_1im}][\mathrm{BF_4}]$), the $T_{0.01/10\,\mathrm{h}}$ of $[\mathrm{C_2C_1im}][\mathrm{OTF}]$ is assumed to be 454 K to ensure the thermal stability of the IL. Consequently, the T_{reboiler} of the first and second extractive distillation columns (334.8 and 433.7 K) is maintained based on P_{column} to be below the known and hypothesized $T_{0.01/10\,\mathrm{h}}$ for $[\mathrm{C_4C_1im}][\mathrm{PF_6}]$ and $[\mathrm{C_2C_1im}][\mathrm{OTF}]$ (<531 and 454 K, respectively).

In most of these cases, transport data is not available, and the rate-based model simulation in the absence of experimental transport data may result in under- or overestimating the size of the equipment. For example, the viscosity of HFC-134a/ $\left[C_6C_1\text{im}\right]\left[Tf_2N\right]$ was estimated with and without experimental data by Zhang et al., as shown in Figure 8. The absence of experimental viscosity data leads to a significant underestimation of the mixture viscosity, which would result in an underestimation of the equipment size (i.e., an overestimation of

Table 4. Summary of the Operating Conditions and Energy Demand for the Selected ILs

refrigerant mixture	R-450A	R-456A ^a		R-515B	R-516A ^a		R-513A ²²
distillation	extractive	extractive	fractional	extractive	extractive -1	extractive -2	extractive
ionic liquid	$[C_2C_1im][BF_4]$	$[C_2C_1im][BF_4]$	N/A	[P _{6,6,6,14}][Cl]	$[C_4C_1im][PF_6]$	$[C_2C_1im][OTF]$	$[C_2C_1im][Ac]$
solvent-to-feed ratio	12.7	12	N/A	3.3	3.5	8	3
number of stages	60	60	30	20	19	40	20
feed stage	30	25	15	10	11	17	13
reflux ratio	5	5	5	2	5	5	2.2
operating pressure [MPa]	2.5	2.5	0.4	0.12	0.5	1.3	0.7
reboiler temperature [K]	454.5	424.8	252.8	436.5	334.8	433.7	333.9
condenser temperature [K]	363.3	363.3	282.17	258.2	287.5	322.6	299.0
reboiler heat duty [kW]	10.58	7.81	0.32	3.51	2.21	1.38	1.3
condenser heat duty [kW]	-0.47	-0.40	-0.36	-1.51	-1.85	-0.23	-0.62
cooler heat duty [kW] ⁻¹	-9.9	-7.4	-0.89	-2.50	-0.39	-0.99	-0.82
cooler heat duty [kW] ⁻²	N/A	N/A	N/A	N/A	N/A	-0.37	N/A
flash tank net duty	0	0	0	0	0	0	0.39
pump and/or compressor network [kW]	0.36	0.33	0.42	0.005	0.012	0.19	0.05
overall absolute energy demand [kW]	21.31	15.94	1.99	7.52	4.46	3.16	3.18
distillate product purity wt %	99.67%	99.55%	99.83%	99.83%	99.85%	97.8%	99.7%
second product purity wt %	99.55%		99.5%	98.3%		97.7%	99.5%
a=		111 .	_	1.0 . 1.			

^aTernary mixtures require two consecutive extractive distillations or extractive and fraction distillation columns.

the mass transport). In this work, the ASPEN Plus simulation is based on equilibrium data; however, transport property measurements are in progress. The equilibrium-based process simulations show that the chosen IL entrainers are effective at separating the refrigerant mixtures using extractive distillation. Equilibrium-based results can be used as a preliminary screening and provide guidance to experimentalists verifying the results.

RESULTS AND DISCUSSION

This work demonstrates the potential of employing extractive distillation with an IL entrainer to separate azeotropic refrigerant mixtures. However, the limited IL solubility data, coupled with the lack of highly selective ILs, necessitates, in some cases, extreme conditions for effective separation (e.g., 60 equilibrium stages, S/F = 12.0-12.7, $P_{\text{column}} = 2.5$ MPa) of refrigerant mixtures R-450A and R-456A as shown in Figures 4 and 5 and Table 4. While a slight increase in stage P enhances the separation of R-515B, it also increases the $T_{\rm reboiler}$ and could potentially increase the level of IL decomposition. To address this, utilizing a more selective and thermally stable IL, especially for HFC-227ea and HFO-1234ze(E), would facilitate achieving ≥99.5 wt % purity for R-515B components. In the case of R-516A, extracting HFO-1234yf in the first extractive distillation proves comparatively easy due to the high solubility of HFC-134a and HFC-152a in [C₄C₁im][PF₆], combined with the lower HFO-1234yf solubility. This shows the significance of finding highly selective ILs, especially for HFO-1234ze(E), which is a component in three of the refrigerant blends studied in this work (e.g., R-450A, R-456A, and R-515).

The ILs as entrainers in extractive distillation exhibit the ability to separate azeotropic refrigerant mixtures into highpurity components. The extreme conditions for separating R-450A and R-456A, in contrast to R-515B and R-516A, arise from low refrigerant solubility and selectivity; ⁵³ however, the S/F and RR ratios were within reasonable ranges for extractive distillation processes. In comparison with our previous work on the separation of R-513A, the operating conditions are S/F ratio = 3, $P_{\rm column}$ = 0.7 MPa, $N_{\rm T}$ = 20 $T_{\rm reboiler}$ = 333.9 K, $T_{\rm condenser}$ = 299.0 K, $P_{\rm flash}$ of 0.01 MPa (0.1 bar), and $T_{\rm flash}$ = 345.15 K. The flash tank,

in contrast to the adiabatic flash operation assumed in this simulation, was operated under isothermal conditions with a specific T and P. This operational difference introduced an additional heat duty to the flash tank. Moreover, the previous study omitted the consideration of low pump work, a factor that was incorporated in the present work for the purpose of comparative analysis. The overall energy demand of the fractional distillation for separating HFC-134a and HFO-1234yf, including the reboiler (1.3 kW), the condenser (-0.62kW), the inlet stream cooler (-0.82 kW), pump work (0.05 kW), and flash duty (0.39 kW), is 3.18 kW. The total energy input, including both extractive and fractional distillations, for separating R-513A into pure components, is 3.18 kW/10 kg/s refrigerant flow rate (0.318 kJ/kg R-513A). The pursuit of superior ILs (i.e., high refrigerant absorption capacity, high selectivity, high thermal stability, and low viscosity) is an interesting optimization problem for facilitating the separation of azeotropic refrigerant mixtures in order to minimize energy consumption, environmental impact, and operating costs, enabling a smooth transition to next-generation refrigerants. Additional experimental measurements and modeling are needed for developing process simulations using ILs.

CONCLUSIONS

Extractive distillation with IL entrainers has demonstrated the potential for effective and efficient separation of azeotropic and near-azeotropic mixtures. The separation processes are designed and simulated based on ASPEN Plus supported with phase equilibrium and critical property data. A targeted purity of ≥ 99.5 wt % was successfully attained for all components in R-450A and R-456A. Despite the low selectivity of ILs for HFC-32, HFC-134a, and HFO-1234ze(E), $[C_2C_1\mathrm{im}][BF_4]$ effectively extracted HFO-1234ze(E) from R-450A and R-456A with the desired purity. The observed lower selectivity can be attributed to specific operating conditions and structural requirements, necessitating a higher number of stages. This limitation, coupled with the thermal stability constraints of ILs, imposes restrictions on process optimization, particularly when operating at or below certain pressures, as exemplified in the separation of R-515B

using [P_{6,6,6,14}][Cl]. This separation demonstrated effective purification of HFC-227ea and HFO-1234ze(E) with purities of 98.3 and 99.83 wt %, respectively, which were also below thermal stability constraints. In the case of R-516A, [C₄C₁im]-[PF₆] and [C₂C₁im][OTF] were utilized to separate the refrigerant mixture into pure components. The higher selectivity of $[C_4C_1\text{im}][PF_6]$ provided the high purity extraction of HFO-1234yf (99.85 wt %), while $[C_2C_1\text{im}][OTF]$ was utilized to separate HFC-134a and HFC-152a, achieving approximately 97 wt % purity for both components. The higher operating conditions and the physical structure of the unit, dictated by the lower selectivity, could contribute to an increase in capital costs. These costs encompass not only unit construction but also expenses associated with overall absolute energy demand. Consequently, the search for superior ILs becomes essential, as they hold the potential to simplify the separation process for the current refrigerant mixtures, thereby minimizing their environmental impact. Such advancements would facilitate a smoother transition to the next-generation refrigerants.

ASSOCIATED CONTENT

Solution Supporting Information

The Supporting Information is available free of charge at https://pubs.acs.org/doi/10.1021/acs.iecr.4c00531.

The Supporting Information contains additional ionic liquid properties, chemical structures, and abbreviations. Vapor—liquid equilibria (VLE) and liquid—liquid equilibria (LLE) modeling, binary interaction parameters between refrigerants and ILs, AAD between estimated and measured values, and ideal gas heat capacities as a function of temperature for ILs are also provided. Finally, a liquid mixture viscosity model is included for future rate-based ASPEN simulations (PDF)

AUTHOR INFORMATION

Corresponding Author

Mark B. Shiflett — Wonderful Institute for Sustainable Engineering, University of Kansas, Lawrence, Kansas 66045, United States; Department of Chemical and Petroleum Engineering, University of Kansas, Lawrence, Kansas 66045, United States; orcid.org/0000-0002-8934-6192; Email: Mark.B.Shiflett@ku.edu

Authors

Abdulrhman M. Arishi — Wonderful Institute for Sustainable Engineering, University of Kansas, Lawrence, Kansas 66045, United States; Department of Chemical and Petroleum Engineering, University of Kansas, Lawrence, Kansas 66045, United States; Department of Chemical Engineering, Jazan University, Jazan 82822, Saudi Arabia; orcid.org/0009-0001-9482-0143

Julia E. Espinoza Mejia — Wonderful Institute for Sustainable Engineering, University of Kansas, Lawrence, Kansas 66045, United States; Department of Chemical and Petroleum Engineering, University of Kansas, Lawrence, Kansas 66045, United States; orcid.org/0000-0002-6646-4276

Complete contact information is available at: https://pubs.acs.org/10.1021/acs.iecr.4c00531

Notes

The authors declare no competing financial interest.

REFERENCES

- (1) EPA, U. Proposed Rule— Phasedown of Hydrofluorocarbons: Establishing the Allowance Allocation and Trading Program under the AIM Act
- (2) Designation and Safety Classification of Refrigerants. ANSI/ASHRAE Standard 34–2007, 2010.
- (3) Update on New Refrigerants Designations and Safety Classifications. ANSI/ASHRAE Standard 34–2023, 2023.
- (4) IPCC 6th Assessment Report; Climate Change 2021, The Physical Science Basis 2021. https://www.ipcc.ch/report/ar6/wg1/ (accessed Jan 22, 2024).
- (5) Honeywell. R-450A Technical Data Sheet. https://www.honeywell-refrigerants.com/europe/product/solstice-n13/ (accessed Jan 22, 2024).
- (6) Honeywell. R-515B Technical Data Sheet. https://www.honeywell-refrigerants.com/europe/product/solstice-n15-r-515b/(accessed Jan 22, 2024).
- (7) Koura. R-456A Technical Data Sheet. https://www.klea.com/next-gen-refrigerants/r456a/#dl-docs (accessed Jan 22, 2024).
- (8) Arkema. R-516A Refrigerant. https://forane.arkema.com/en/forane-refrigerants/next-generation-products-hvac-hfo/ (accessed Jan 22, 2024).
- (9) Gatarić, P.; Lorbek, L. Evaluating R450A as a drop-in replacement for R134a in household heat pump tumble dryers. *Int. J. Refrig.* **2021**, 128, 22–33.
- (10) Makhnatch, P.; Mota-Babiloni, A.; Khodabandeh, R. Experimental study of R450A drop-in performance in an R134a small capacity refrigeration unit. *Int. J. Refrig.* **2017**, *84*, 26–35.
- (11) Mota-Babiloni, A.; Mateu-Royo, C.; Navarro-Esbrí, J.; Barragán-Cervera, Á. Experimental comparison of HFO-1234ze(E) and R-515B to replace HFC-134a in heat pump water heaters and moderately high temperature heat pumps. *Appl. Therm Eng.* **2021**, *196*, No. 117256.
- (12) Kim, S.; Crosby, K.; Rodowski, D. Very Low GWP Refrigerant R-516A for R-134a replacement in Commercial Refrigeration" (2021). International Refrigeration and Air Conditioning Conference. Paper 2147https://docs.lib.purdue.edu/iracc/2147.
- (13) Méndez-Méndez, D.; Pérez-García, V.; Morales-Fuentes, A. Experimental energy evaluation of R516A and R513A as replacement of R134a in refrigeration and air conditioning modes. *Int. J. Refrig.* **2023**, 154, 73–83
- (14) Chemours, Opteon XP10 (R-513A) Refrigerant. https://www.opteon.com/en/products/refrigerants/xp10 (accessed Jan 22, 2024).
- (15) Zaitsau, D. H.; Kabo, G. J.; Strechan, A. A.; Paulechka, Y. U.; Tschersich, A.; Verevkin, S. P.; Heintz, A. Experimental Vapor Pressures of 1-Alkyl-3-methylimidazolium Bis-(trifluoromethylsulfonyl)imides and a Correlation Scheme for Estimation of Vaporization Enthalpies of Ionic Liquids. *J. Phys. Chem. A* 2006, 110 (22), 7303-7306.
- (16) Wasserscheid, P.; Keim, W. Ionic Liquids—New "Solutions" for Transition Metal Catalysis. *Angew. Chem., Int. Ed.* **2000**, 39 (21), 3772—2780
- (17) Chen, Y.; Cao, Y.; Shi, Y.; Xue, Z.; Mu, T. Quantitative Research on the Vaporization and Decomposition of [EMIM][Tf2N] by Thermogravimetric Analysis—Mass Spectrometry. *Ind. Eng. Chem. Res.* **2012**, *51* (21), 7418—7427.
- (18) Meine, N.; Benedito, F.; Rinaldi, R. Thermal stability of ionic liquids assessed by potentiometric titration. *Green Chem.* **2010**, *12* (10), 1711–1714.
- (19) Cao, Y.; Mu, T. Comprehensive Investigation on the Thermal Stability of 66 Ionic Liquids by Thermogravimetric Analysis. *Ind. Eng. Chem. Res.* **2014**, 53 (20), 8651–8664.
- (20) Deferm, C.; Van den Bossche, A.; Luyten, J.; Oosterhof, H.; Fransaer, J.; Binnemans, K. Thermal stability of trihexyl(tetradecyl)-phosphonium chloride. *Phys. Chem. Chem. Phys.* **2018**, 20 (4), 2444–2456
- (21) Wooster, T. J.; Johanson, K. M.; Fraser, K. J.; MacFarlane, D. R.; Scott, J. L. Thermal degradation of cyano containing ionic liquids. *Green Chem.* **2006**, *8* (8), 691–696.

- (22) Arishi, A. M.; Shiflett, M. B. Azeotropic Refrigerant Mixture R-513A Separation Using Extractive Distillation with Ionic Liquids Entrainers. *Ind. Eng. Chem. Res.* **2023**, *62* (46), 19862–19872.
- (23) Liu, X.; Bai, L.; Liu, S.; He, M. Vapor–Liquid Equilibrium of R1234yf/[HMIM][Tf2N] and R1234ze(E)/[HMIM][Tf2N] Working Pairs for the Absorption Refrigeration Cycle. *J. Chem. Eng. Data* **2016**, *61* (11), 3952–3957.
- (24) Liu, X.; Pan, P.; Yang, F.; He, M. Solubilities and diffusivities of R227ea, R236fa and R245fa in 1-hexyl-3-methylimidazolium bis-(trifluoromethylsulfonyl)imide. *J. Chem. Thermodyn.* **2018**, *123*, 158–164.
- (25) Sun, Y.; Wei, Q.; Wang, X.; Wang, X.; He, M. Absorption Separation of Hydrofluorocarbon/Hydrofluoroolefin Refrigerant Mixtures Using Ionic Liquids. *Ind. Eng. Chem. Res.* **2022**, *61* (34), 12787–12796.
- (26) Jiang, T.; Meng, X.; Sun, Y.; Jin, L.; Wei, Q.; Wang, J.; Wang, X.; He, M. Absorption behavior for R1234ze(E) and R1233zd(E) in [P66614][Cl] as working fluids in absorption refrigeration systems. *Int. J. Refrig.* **2021**, *131*, 178–185.
- (27) Viar, M.; Asensio-Delgado, S.; Pardo, F.; Zarca, G.; Urtiaga, A. In the quest for ionic liquid entrainers for the recovery of R-32 and R-125 by extractive distillation under rate-based considerations. *Sep. Purif. Technol.* **2023**, 324, No. 124610.
- (28) Sanmamed, Y. A.; González-Salgado, D.; Troncoso, J.; Romani, L.; Baylaucq, A.; Boned, C. Experimental methodology for precise determination of density of RTILs as a function of temperature and pressure using vibrating tube densimeters. *J. Chem. Thermodyn.* **2010**, 42 (4), 553–563.
- (29) Harris, K. R.; Woolf, L. A.; Kanakubo, M. Temperature and Pressure Dependence of the Viscosity of the Ionic Liquid 1-Butyl-3-methylimidazolium Hexafluorophosphate. *J. Chem. Eng. Data* **2005**, *S0* (5), 1777–1782.
- (30) Kou, L.; Yang, Z.; Tang, X.; Zhang, W.; Lu, J. Experimental measurements and correlation of isothermal vapor-liquid equilibria for HFC-32 + HFO-1234ze (E) and HFC-134a + HFO-1234ze (E) binary systems. *J. Chem. Thermodyn.* **2019**, *139*, No. 105798.
- (31) Holcomb, C. D.; Magee, J. W.; Scott, J. L.; Haynes, W.; Outcalt, S. Selected thermodynamic properties for mixtures of r-32 (difluoromethane), r-125 (pentafluoroethane), r-134a (1, 1, 1, 2-tetrafluoroethane), r-143a (1, 1, 1-trifluoroethane), r-41 (fluoromethane), r-290 (propane), and r-744 (carbon dioxide). Technical Note; National Inst. of Standards and Technology: Boulder, CO, 1997.
- (32) Kleiber, M. Vapor-liquid equilibria of binary refrigerant mixtures containing propylene or R134a. *Fluid Phase Equilib.* **1994**, 92, 149–194.
- (33) Hu, P.; Chen, L.-X.; Zhu, W.-B.; Jia, L.; Chen, Z.-S. Isothermal VLE measurements for the binary mixture of 2,3,3,3-tetrafluoroprop-1-ene (HFO-1234yf)+1,1-difluoroethane (HFC-152a). *Fluid Phase Equilib.* **2014**, 373, 80–83.
- (34) Kamiaka, T.; Dang, C.; Hihara, E. Vapor-liquid equilibrium measurements for binary mixtures of R1234yf with R32, R125, and R134a. *Int. J. Refrig.* **2013**, *36* (3), 965–971.
- (35) Abbadi, J. E.; Coquelet, C.; Valtz, A.; Houriez, C. Experimental measurements and modelling of vapour—liquid equilibria for four mixtures of 2,3,3,3—tetrafluoropropene (R1234yf) with 1,1,1,2—tetrafluoroethane (R134a) or 1,1—difluoroethane (R152a) or trans—1—chloro—3,3,3—trifluoropropene (R1233zd(E)) or 2—chloro—3,3,3—trifluoropropene (R1233xf). *Int. J. Refrig.* 2022, 140, 172—185.
- (36) Asensio-Delgado, S.; Pardo, F.; Zarca, G.; Urtiaga, A. Machine learning for predicting the solubility of high-GWP fluorinated refrigerants in ionic liquids. *J. Mol. Liq.* **2022**, *367*, No. 120472, DOI: 10.1016/j.molliq.2022.120472.
- (37) Mathias, P. M.; Klotz, H. C.; Prausnitz, J. M. Equation-of-State mixing rules for multicomponent mixtures: the problem of invariance. *Fluid Phase Equilib.* **1991**, *67*, 31–44.
- (38) Peng, D.-Y.; Robinson, D. B. A New Two-Constant Equation of State. *Ind. Eng. Chem. Fundam.* **1976**, *15* (1), 59–64.
- (39) Boston, J. F.; Mathias, P.Phase Equilibria in a Third-Generation Process Simulator. In *EFCE Publication Series (European Federation of Chemical Engineering)* 1980; pp 823–849.

- (40) Maqbool, W.; Dunn, K.; Doherty, W.; McKenzie, N.; Hobson, P. Solubility of benzyl alcohol in supercritical carbon dioxide, comparison of literature data and thermodynamic modelling. *Chem. Eng. Process.* **2020**, *151*, No. 107907.
- (41) Asensio-Delgado, S.; Pardo, F.; Zarca, G.; Urtiaga, A. Vapor–Liquid Equilibria and Diffusion Coefficients of Difluoromethane, 1,1,1,2-Tetrafluoroethane, and 2,3,3,3-Tetrafluoropropene in Low-Viscosity Ionic Liquids. *J. Chem. Eng. Data* **2020**, *65* (9), 4242–4251.
- (42) Sun, Y.; Zhang, Y.; Wang, X.; Prausnitz, J. M.; Jin, L. Gaseous absorption of 2,3,3,3-tetrafluoroprop-1-ene in three imidazolium-based ionic liquids. *Fluid Phase Equilib.* **2017**, *450*, *65*–74.
- (43) Shiflett, M. B.; Yokozeki, A. Solubility and diffusivity of hydrofluorocarbons in room-temperature ionic liquids. *AIChE J.* **2006**, *52* (3), 1205–1219.
- (44) Shiflett, M. B.; Yokozeki, A. Vapor—Liquid—Liquid Equilibria of Hydrofluorocarbons + 1-Butyl-3-methylimidazolium Hexafluorophosphate. *J. Chem. Eng. Data* **2006**, *S1* (5), 1931—1939.
- (45) Ren, W.; Scurto, A. M. Phase equilibria of imidazolium ionic liquids and the refrigerant gas, 1,1,1,2-tetrafluoroethane (R-134a). *Fluid Phase Equilib.* **2009**, 286 (1), 1–7.
- (46) Wang, X.; Zhang, Y.; Wang, D.; Sun, Y. Phase Equilibria of trans-1,3,3,3-Tetrafluoropropene with Three Imidazolium Ionic Liquids. *J. Chem. Eng. Data* **2017**, *62* (6), 1825–1831.
- (47) Sun, Y.; Zhang, Y.; Di, G.; Wang, X.; Prausnitz, J. M.; Jin, L. Vapor–Liquid Equilibria for R1234ze(E) and Three Imidazolium-Based Ionic Liquids as Working Pairs in Absorption–Refrigeration Cycle. *J. Chem. Eng. Data* **2018**, *63* (8), 3053–3060.
- (48) Asensio-Delgado, S.; Pardo, F.; Zarca, G.; Urtiaga, A. Vapor-Liquid Equilibria and Diffusion Coefficients of Difluoromethane, 1,1,1,2-Tetrafluoroethane, and 2,3,3,3-Tetrafluoropropene in Low-Viscosity Ionic Liquids. *J. Chem. Eng. Data* **2020**, *65* (9), 4242–4251.
- (49) Ge, R.; Hardacre, C.; Jacquemin, J.; Nancarrow, P.; Rooney, D. W. Heat capacities of ionic liquids as a function of temperature at 0.1 MPa. measurement and prediction. *J. Chem. Eng. Data* **2008**, 53 (9), 2148–2153.
- (50) Valderrama, J. O.; Rojas, R. E. Critical Properties of Ionic Liquids. Revisited. *Ind. Eng. Chem. Res.* **2009**, 48 (14), 6890–6900.
- (51) Sattari, M.; Kamari, A.; Mohammadi, A. H.; Ramjugernath, D. On the prediction of critical temperatures of ionic liquids: Model development and evaluation. *Fluid Phase Equilib.* **2016**, *411*, 24–32.
- (52) Ayuso, M.; Cañada-Barcala, A.; Larriba, M.; Navarro, P.; Delgado-Mellado, N.; García, J.; Rodríguez, F. Enhanced separation of benzene and cyclohexane by homogeneous extractive distillation using ionic liquids as entrainers. *Sep. Purif. Technol.* **2020**, 240, No. 116583.
- (53) Finberg, E. A.; Shiflett, M. B. Process Designs for Separating R-410A, R-404A, and R-407C Using Extractive Distillation and Ionic Liquid Entrainers. *Ind. Eng. Chem. Res.* **2021**, *60* (44), 16054–16067.
- (54) Finberg, E. A.; May, T. L.; Shiflett, M. B. Multicomponent Refrigerant Separation Using Extractive Distillation with Ionic Liquids. *Ind. Eng. Chem. Res.* **2022**, *61* (27), 9795–9812.
- (55) Cao, Y. Y.; Mu, T. C. Comprehensive Investigation on the Thermal Stability of 66 Ionic Liquids by Thermogravimetric Analysis. *Ind. Eng. Chem. Res.* **2014**, 53 (20), 8651–8664.
- (56) Heym, F.; Korth, W.; Thiessen, J.; Kern, C.; Jess, A. Evaporation and Decomposition Behavior of Pure and Supported Ionic Liquids under Thermal Stress. *Chem. Ing. Tech.* **2015**, *87* (6), 791–802.
- (57) Zhang, Y.; Wang, X.; Yin, J. Viscosity of saturated mixtures of 1-hexyl-3-methyl-imidazolium bis(trifluoromethylsulfonyl)amide with R600a and R152a. *J. Chem. Thermodyn.* **2020**, *141*, No. 105970.